

Further reactions of some bis(vinylidene)diruthenium complexes

Michael I. Bruce^{a,*}, Benjamin G. Ellis^a, Brian W. Skelton^b, Allan H. White^b

^a Department of Chemistry, University of Adelaide, Adelaide, SA 5005, Australia

^b Department of Chemistry, University of Western Australia, Crawley, WA 6009, Australia

Received 19 August 2004; accepted 29 September 2004

Available online 10 December 2004

Abstract

Whereas $\{\text{Ru}(\text{dppm})\text{Cp}^*\}_2(\mu\text{-C}\equiv\text{C}\equiv\text{C})$ (**2**) is the only product formed by deprotonation of $[\{\text{Ru}(\text{dppm})\text{Cp}^*\}_2\{\mu(\text{=C=CHCH=C=})\}]^+$ with dbu, a mixture of **2** with $\text{Ru}\{\text{C}\equiv\text{CCH=CH}(\text{PPh}_2)_2[\text{RuCp}^*]\}(\text{dppm})\text{Cp}^*$ (**3**) and $\{\text{Cp}^*\text{Ru}(\text{PPh}_2\text{CHC=CH-})_2$ (**4**) is obtained with KOBU^t . A similar reaction with $[\{\text{Ru}(\text{dppm})\text{Cp}^*\}_2\{\mu(\text{=C=CMeCMe=C=})\}]^+$ (**5**) gave $\text{Ru}\{\text{C}\equiv\text{CCMe=CH}(\text{PPh}_2)_2[\text{RuCp}^*]\}(\text{dppm})\text{Cp}^*$ (**6**). X-ray structures of **4**, **5** and **6** confirm the presence of the 1-ruthena-2,4-diphosphabicyclo[1.1.1]pentane moiety, which is likely formed by an intramolecular attack of the deprotonated dppm ligand on C(1) of the vinylidene ligand. Protonation of $\{\text{Ru}(\text{dppe})\text{Cp}^*\}_2(\mu\text{-C}\equiv\text{C}\equiv\text{C})$ (**8-Ru**) regenerates its precursor $[\{\text{Ru}(\text{dppe})\text{Cp}^*\}_2\{\mu(\text{=C=CHCH=C=})\}]^{2+}$ (**7-Ru**). Ready oxidation of the bis(vinylidene) complex affords the cationic carbonyl $[\text{Ru}(\text{CO})(\text{dppe})\text{Cp}^*]\text{PF}_6$ (**9**) (X-ray structure).

© 2004 Elsevier B.V. All rights reserved.

1. Introduction

The diynydiyl complexes of the Group 8 metals continue to be a source of novel chemistry [1], while complexes containing C_4 chains end-capped by $\text{M}(\text{PP})\text{Cp}'$ [$\text{M} = \text{Fe}, \text{Ru}, \text{Os}$; $\text{PP} = (\text{PPh}_3)_2, \text{dppm}, \text{dppe}$; $\text{Cp}' = \text{Cp}, \text{Cp}^*$] have been shown to undergo a variety of redox processes which suggest that electronic communication (hole/electron transfer) between the two metal centres occurs rather efficiently through the carbon chain [2–4]. Among the precursors of these complexes are the related bis(vinylidene) complexes, generally obtained by oxidative coupling of the analogous ethynyl derivatives, and compounds containing $\text{M}-\text{C}_4-\text{R}$ [$\text{R} = \text{H}, \text{SiMe}_3, \text{Au}(\text{PR}'_3)$] fragments [5].

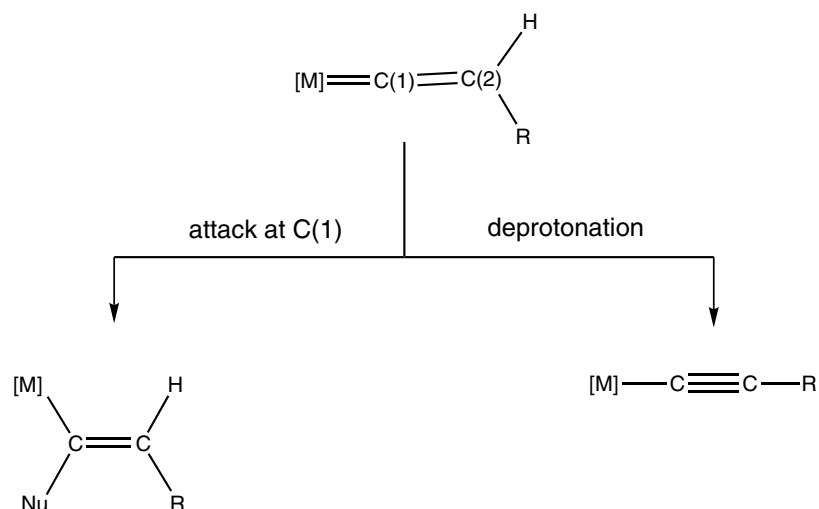
In turn, the chemistry of transition-metal vinylidene complexes is well understood having been the subject of experimental and theoretical studies which are sum-

marised in a number of reviews [6–8]. Calculations have shown that the reactivity of these complexes is directed by the electronic properties of the vinylidene ligand [9]. In general, C_1 is electron poor and subject to attack by nucleophiles [2b,10,11]. However, in mono- or unsubstituted vinylidenes, the vinylic proton is acidic and as a consequence competition occurs between nucleophilic attack at C(1) and deprotonation to form the corresponding alkynyl complex (Scheme 1) [6,7].

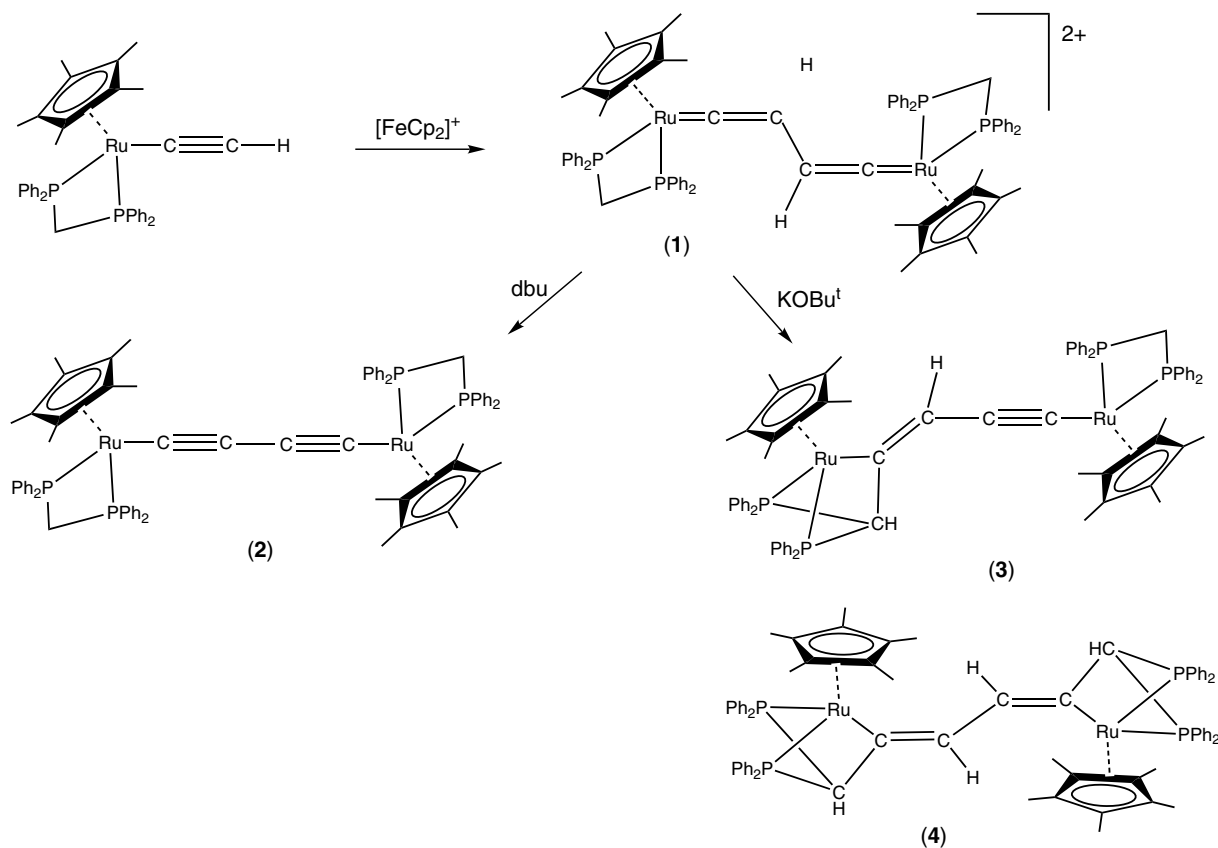
In the course of studies on the bis(vinylidene) complex precursor $[\{\text{Ru}(\text{dppm})\text{Cp}^*\}_2\{\mu(\text{=C=CHCH=C=})\}](\text{PF}_6)_2$ (**1**), formed by oxidative coupling of the analogous ethynyl complex (Scheme 2), we have uncovered alternative reaction routes. While we and others have reported suitable conditions for the deprotonation of analogous bis(vinylidene) complexes to proceed in reasonable yield [2b,3b], when examining similar reactions of **1**, we discovered that the choice of base was crucial to the success of the reaction. In this paper, we describe the formation and characterisation of these alternative products.

* Corresponding author. Tel.: +61 8 8303 5939; fax: +61 8 8303 4358.

E-mail address: michael.bruce@adelaide.edu.au (M.I. Bruce).



Scheme 1.



Scheme 2.

2. Results and discussion

2.1. Reaction of $[\{ Ru(dppm)Cp^* \}_2 \{ \mu-(=C=CHCH=C=) \}] (PF_6)_2$ (**1**) with $KOBu^t$

Whereas deprotonation of the bis(vinylidene) complex $[\{ Cp^*(dppm)Ru \}_2 (\mu-C=CHCH=C)] (PF_6)_2$ (**1**)

with dbu afforded $\{ Ru(dppm)Cp^* \}_2 (\mu-C\equiv CC\equiv C)$ (**2**) as the sole product [3b], use of $KOBu^t$ resulted in the formation of a mixture of **2** (35%) with two other products identified as $Ru\{C\equiv CCH=CCH(PPh_2)_2\} [RuCp^*]$ ($dppm$) Cp^* (**3**) (60%) and the symmetrical $\{ Ru[(PPh_2)_2-CHC=CH-C]Cp^* \}_2$ (**4**) (5%) (Scheme 2). The presence of the three complexes in the mixture was shown in the ^{31}P

NMR spectrum which, in addition to a resonance for **2** at δ 16.63 [3b], had two equal intensity singlets at δ -1.79 and 18.99 (assigned to **3**), together with a lower intensity peak at δ -3.06 (for **4**). In the ^1H NMR spectrum, several resonances assigned to the various Cp* methyl groups, which had relative intensities matching those of the ^{31}P signals, were found at δ 1.90 (for **2**), 1.98 and 2.07 (**3**; both triplets), and 2.24 (**4**). The simple spectrum for **4** is consistent with the solid-state symmetrical structure, while the two sets of resonances in **3** are assigned to the intact dpmm and the bicyclic ligands, respectively, by comparison with **2** and **4**, and are consistent with the asymmetric structure shown. Other resonances in the ^1H NMR spectra are characteristic of the dpmm CH_2 groups [unresolved multiplets at δ 4.22 (**2**) and 4.12 (**3**)] and the CH protons of the bicyclic ligands [broad resonances at δ 5.59 (**3**) and 6.43 (**4**)]. In **3**, the $=\text{CH}$ proton of the substituted vinyl groups gives rise to a singlet at δ 2.11, but the vinylic protons of **4** were not observed.

All attempts to obtain single crystals of **3** suitable for X-ray diffraction have been unsuccessful, only very thin fibres being formed. However, the proposed structure of **4** was confirmed when single crystals suitable for X-ray diffraction studies could be separated by hand from the mixture with **3**. Two independent molecules with quasi- $2/m$ symmetry are present in the unit cell, one of these (mol. 2) actually being centrosymmetric [Fig. 1(a); selected structural parameters are given in Table 1]. The organic ligand is a substituted vinyl group and the Ru–C(1)–C(2) angles have decreased to between $135.6(9)$ and $139(1)^\circ$. Atoms Ru(n 1)–P(n 1, n 2)–C(11, 12) [or C(15, 16) in the second half of the molecule] form a 1-ruthena-2,4-diphosphabicyclo[1.1.1]pentane system, which results in smaller than normal P–Ru–P [70.9 – $71.1(1)^\circ$] and P–Ru–C [63.6 – $64.8(3)^\circ$] angles. Angles at atoms in the carbon chain range between 124° and $130(1)^\circ$, somewhat larger than the 120° expected for $\text{C}(\text{sp}^2)$ atoms. As a whole, the C_4 chain has a *transoid* conformation, resulting in a separation of $7.761(2)/7.797(2)$ Å between the two ruthenium atoms. The torsion angles between the Ru–Cp* axes are $-177.6^\circ/180^\circ$. The significant deviation from linearity across Ru–C(1)–C(2) (ca. 135°) is the result of the C(1)–C(2) double bond linking the C_4 chain. The C(1)–C(2) double bond has a typical length of $1.37(2)$ Å and is coplanar with its substituents [Ru(1), C(11), C(3)]. The Ru–C(1) bond [$2.11(1)$ Å] is longer than those found in the related vinylidene [Ru(=C=CH₂)(dpmm)Cp*]PF₆ [$1.848(2)$ Å] [3b] or diyndiyl **2** [$2.017(2)$ Å] [3b] complexes, but is typical for a Ru–C(sp²) bond, e.g. $2.103(6)$ Å in Ru{C(O–Prⁱ)=CHPh}(CO)(PPh₃)Cp [12].

The molecular structure suggests that **3** and **4** arise by intramolecular attack of the deprotonated dpmm ligand(s) (structure **A** in Scheme 3) at C(1) of the vinylidene to give tricyclic 4/4/5 systems centred on

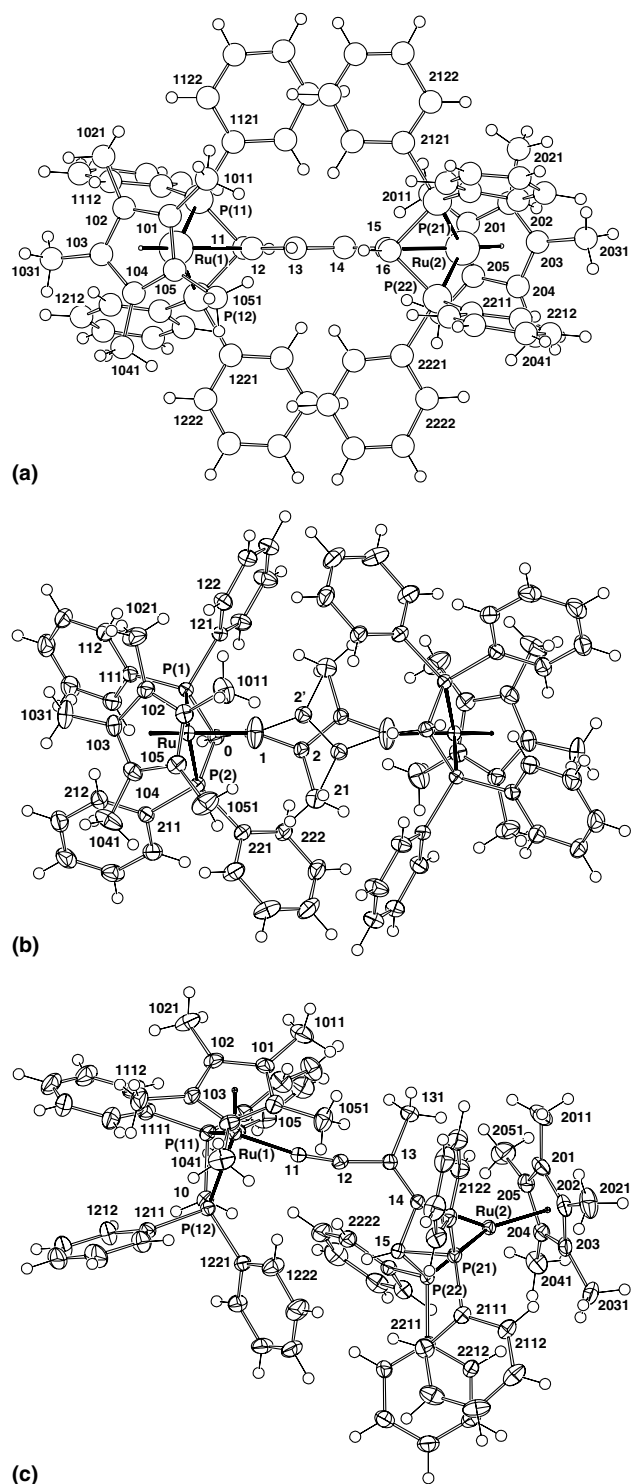


Fig. 1. Projections of: (a) molecule 1 of $\{\text{Cp}^*\text{Ru}(\text{PPh}_2\text{CHC}=\text{CH}-)\}_2$ (**4**) through its *pseudo*-mirror plane, normal to the quasi- 2 -axis; (b) the cation of $[\{\text{Ru}(\text{dppe})\text{Cp}^*\}_2\{\mu(\text{C}=\text{CMeCMe}=\text{C}=\text{C})\}]\text{OTf}$ (**5**) projected approximately normal to the central hydrocarbon plane, the minor component of the latter being shown with single line bonds; (c) molecule 1 of $\{\text{Cp}^*(\text{dpmm})\text{Ru}\}\{\mu\text{-C}\equiv\text{CCMe}=\text{CCH}(\text{PPh}_2)_2\}\{\text{RuCp}^*\}$ (**6**).

each ruthenium. Similar complexes have been described on previous occasions by several groups [13–15].

Table 1
Selected bond distances (Å) and angles (°)

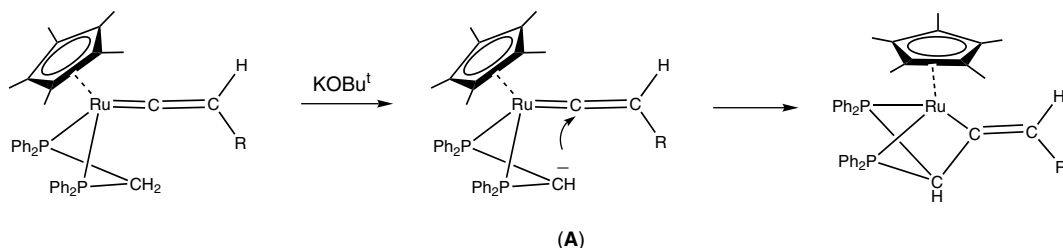
Compound	4 ^a	5	6 ^a
<i>Bond distances (Å)</i>			
Ru(1)–P(11)	2.281(4), 2.289(4)	2.3189(6)	2.2662(8), 2.2578(8)
Ru(1)–P(12)	2.271(4), 2.278(4)	2.2979(7)	2.2733(8), 2.2705(8)
Ru(2)–P(21)	2.284(4)		2.2807(7), 2.2826(7)
Ru(2)–P(22)	2.280(4)		2.2723(8), 2.2698(8)
Ru(1)–C(cp)	2.15–2.26(1), 2.15–2.22(1)	2.243–2.293(2)	2.227–2.259(2), 2.234–2.274(2)
(av.)	2.20(4), 2.20(3)	2.27(2)	2.243(13), 2.253(16)
Ru(2)–C(cp)	2.18–2.23(1)		2.217–2.240(3), 2.214–2.244(3)
(av.)	2.21(2)		2.228(10), 2.229(11)
Ru(1)–C(12)	2.11(1), 2.12(1)	1.851(3)	2.024, 2.028(2) [C(11)]
Ru(2)–C(15)	2.10(1)		2.154(2), 2.171(2) [C(14)]
C(11)–C(12)	1.59(2), 1.55(2)	1.377(5)	1.224(3), 1.223(3)
C(12)–C(13)	1.37(2), 1.31(2)	1.432(6) [C(2')]	1.449(3), 1.447(3)
C(2)–C(21)		1.527(6)	1.514(5), 1.518(4) [C(13)–C(131)]
C(13)–C(14)	1.44(2), 1.45(2)		1.357(4), 1.347(3)
C(14)–C(15)	1.37(2)		1.547(4), 1.549(4)
C(15)–C(16)	1.50(2)		
P(11)–C(11)	1.82(1), 1.82(1)	1.840(3) [C(0)]	1.863(3), 1.853(3) [C(0)]
P(12)–C(11)	1.84(1), 1.86(1)	1.839(2) [C(0)]	1.855(3), 1.858(3) [C(0)]
P(21)–C(16)	1.87(1)		1.857(3), 1.853(3)
P(22)–C(16)	1.84(1)		1.839(2), 1.845(2)
<i>Bond angles (°)</i>			
P(11)–Ru(1)–P(12)	71.1(1), 71.0(1)	70.18(2)	71.73(3), 71.37(3)
P(21)–Ru(2)–P(22)	70.9(1)		71.23(3), 71.31(2)
P(11)–Ru(1)–C(12)	64.0(3), 63.8(3)	90.53(9) [C(1)]	85.61(8), 82.68(8)
P(12)–Ru(1)–C(12)	64.3(3), 64.8(3)	82.94(10) [C(1)]	86.07(8), 84.44(8) [C(11)]
P(21)–Ru(2)–C(15)	63.8(3)		63.15(7), 63.11(7) [C(14)]
P(22)–Ru(2)–C(15)	63.6(3)		63.58(7), 63.61(7) [C(14)]
Ru(1)–P(11)–C(11)	83.8(4), 82.8(4)		
Ru(1)–P(12)–C(11)	83.7(4), 82.3(4)		
Ru(2)–P(21)–C(16)	82.2(4)		83.52(7), 83.63(7) [C(15)]
Ru(2)–P(22)–C(16)	82.8(4)		84.15(9), 84.18(9) [C(14)]
Ru(1)–C(12)–C(11)	95.5(7), 95.3(7)	157.7(1)	169.4(2), 171.9(2)
Ru(1)–C(12)–C(13)	135.6(9), 139(1)		
C(11)–C(12)–C(13)	129(1), 125(1)	71.4(4) [C(2')]	171.3(3), 171.7(3)
C(1)–C(2)–C(21)		126.6(3)	115.4(2), 115.1(2) [C(131)]
C(12)–C(13)–C(14)	126(1), 130(1)		123.3(3), 123.3(3)
C(13)–C(14)–C(15)	124(1)		121.7(2), 121.8(2)
C(14)–C(15)–C(16)	127(1)		
Ru(2)–C(15)–C(14)	135.2(9)		142.6(2), 142.9(2)
Ru(2)–C(15)–C(16)	98.1(7)		
P(11)–C(11)–P(12)	92.3(6), 92.4(6)	92.33(9) [C(0)]	
P(21)–C(16)–P(22)	90.9(6)		
P(11)–C(11)–C(12)	85.8(7), 87.2(8)		
P(12)–C(11)–C(12)	85.3(7), 87.2(7)		
P(21)–C(16)–C(15)	86.4(8)		85.6(2), 86.1(2)
P(22)–C(16)–C(15)	86.9(8)		86.7(1), 86.8(1)

^a For Ru(1), P(11, 12), C(11, 12, 13, 14) (second entries), read Ru(3), P(31, 32), C(31, 32, 33, 33'), etc. (in mol. 2) (centrosymmetric).

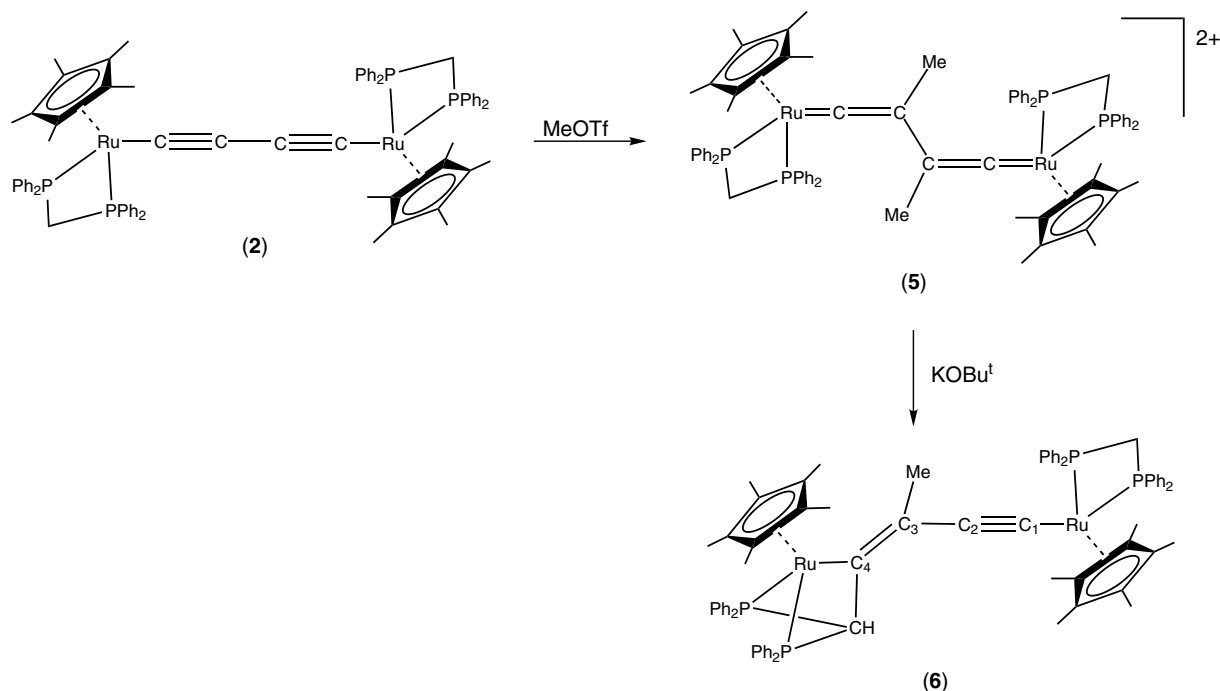
2.2. Synthesis of [$\{\text{Ru}(\text{dppm})\text{Cp}^*\}_2(\text{C}=\text{CMeC}=\text{CMe}=\text{C}=\text{C})\text{C}(\text{OTf})_2$] (**5**)

As the individual products from the reaction between **1** and KOBU^t could not be separated, it was anticipated that deprotonation of the methyl analogue of **1** would favour deprotonation of the dppm ligands to give the methyl analogue of **4**. The isolation and NMR characterisation of this derivative would further support those assignments made for **4**, and hence **3**.

Accordingly, addition of 2.2 equivalents of methyl triflate to a CH_2Cl_2 solution of **1** resulted in a rapid colour change from orange to deep red, before changing further to bright green. The product was crystallised directly by the addition of diethyl ether to the reaction mixture to give [$\{\text{Ru}(\text{dppm})\text{Cp}^*\}_2(\text{C}=\text{CMeC}=\text{CMe}=\text{C}=\text{C})\text{C}(\text{OTf})_2$] (**5**) in 63% yield (Scheme 4). A single band at 1626 cm^{-1} in the IR spectrum of **5** confirmed the bridging C_4 ligand exists as a bis-vinylidene. In the NMR spectra, characteristic resonances for the



Scheme 3.



Scheme 4.

Ru(dppm)Cp* fragment were observed. Interest lies in the upfield signal of the methyl protons, a singlet at δ 0.06. Characteristic resonances for the vinylidene ligand were found in the ^{13}C NMR spectrum at δ 352.20 and 104.61, assigned to atoms C₁ and C₂, respectively. The ES-mass spectrum contained two major ions at m/z 1469 and 660, assigned to $[\text{M} + \text{OTf}]^+$ and M^{2+} , respectively.

Single crystals of **5** suitable for X-ray diffraction were grown by slow evaporation of a concentrated CH_2Cl_2 /hexane solution. A view of the cation in **5** is shown in Fig. 1(b), while selected structural parameters are given in Table 1. As expected, the structure of the centrosymmetric **5** is very similar to that of **1** with the two Cp* ligands adopting a *transoid* arrangement; the gross symmetry is similar to that of **4**, broken by twisting of the central hydrocarbon string to lie quasi-normal to the putative mirror plane. Confirmation of the vinylidene ligand comes with the short Ru–C(1) [1.851(3) Å] and C(1)–C(2) [1.376(5) Å] bonds and longer C(2)–

C(2') bond [1.463(5) Å], all of which are very similar to those found in **1**.

2.3. Deprotonation of $[\{\text{Ru}(\text{dppm})\text{Cp}^*\}_2(=\text{C}=\text{CMeCMe}=\text{C})](\text{OTf})_2$ (**5**)

Treatment of **5** with KOBu^t in THF gave a bright orange solid, NMR and structural data confirming that Ru{C≡CCH=CH(PPh₂)₂[RuCp*]}(dppm)Cp* (**6**) is the sole product from the reaction (Scheme 4). Surprisingly, in this case KOBu^t has deprotonated a single dppm ligand allowing for the formation of the metallacyclopentadiene, as well as removing a methyl group from the vinylidene to give the alkynyl group in **6**. There was no evidence for the formation of the anticipated methyl analogue of **4**.

Spectroscopic features shown by **6** are similar to those observed for **3**. Two bands in the IR spectrum at 1713 and 1950 cm^{-1} are consistent with the presence of both C=C double and C≡C triple bonds. The asym-

metric nature of **6** was confirmed by the two equal intensity resonances at δ 0.49 and 19.05 in the ^{31}P NMR spectrum, assigned to the phosphorus nuclei of the metallacycle and the dppm ligand, respectively. In the ^1H NMR spectrum, two Cp^* resonances appeared at δ 1.97 and 2.22, with the upfield signal assigned to the $\text{Ru}(\text{dppm})\text{Cp}^*$ centre. The CH_2 protons of dppm give broad multiplets at δ 3.94 and 4.25, while the resonance for the $(\text{Ph}_2\text{P})_2\text{CH}$ proton appears as a triplet at δ 5.43. The vinylidene methyl group gives a triplet at δ 1.99.

The ^{13}C NMR spectrum of **6** contains two sets of Cp^* resonances at δ 11.42 and 13.15 (C_5Me_5) and at δ 87.85 and 91.28 (ring carbons). A triplet at δ 27.87 is assigned to the $(\text{Ph}_2\text{P})_2\text{CH}$ group while the $(\text{Ph}_2\text{P})_2\text{CH}_2$ carbon of the dppm ligand gives a triplet at δ 49.79. Resonances for the four carbons bridging the two ruthenium centres are also observed. The resonance for C_1 [δ 116.84] is a well resolved triplet of triplets with a larger coupling [$J(\text{CP})$ 25 Hz] to the phosphorus nuclei of dppm and a smaller coupling [$J(\text{CP})$ 5 Hz] to the two equivalent phosphorus nuclei of the $(\text{Ph}_2\text{P})_2\text{CH}$ ligand. Coupling to dppm is also observed with C_2 , which appeared as a triplet at δ 113.53 [$J(\text{CP})$ 11 Hz]. Atom C_3 gives a triplet at δ 72.54 [$J(\text{CP})$ 23 Hz] by coupling to the $(\text{Ph}_2\text{P})_2\text{CH}$ ligand. The resonance of ruthenium-bound C_4 was shifted significantly downfield to δ 203.24, while the methyl group was found at δ 29.94. In general, NMR data collected for **6** were fully consistent with the assignments made for its hydrogen analogue **3** and both support the proposed structures of these two complexes.

The ES-mass spectrum contains a strong $[\text{M} + \text{H}]^+$ ion centred on m/z 1305 with no other fragmentation observed, even at higher cone voltages. If solutions of **6** in MeOH were left for extended periods of time (days), the colour changed from orange to brown and the ES-MS of this solution contained a $[\text{M} + \text{MeOH}]^+$ ion at m/z 1336, suggesting the change was due to the addition of MeOH to **6**.

Crystals of **6** suitable for X-ray diffraction were grown from a benzene/hexane solution, a single molecule being shown in Fig. 1(c), while selected bond parameters are given in Table 1. The structure confirms the presence of both ethynyl and metallabicyclic fragments attached to the ruthenium atoms. Bond lengths for the ethynyl portion resemble those of $\text{Ru}(\text{C}\equiv\text{CH})(\text{dppm})\text{Cp}^*$ [3b], with those for $\text{Ru}(1)-\text{C}(11)$ [2.024(2) Å] and $\text{C}(11)-\text{C}(12)$ [1.224(3) Å] (values for mol. 1 given) fully consistent with the expected values for $\text{Ru}-\text{C}$ single and $\text{C}\equiv\text{C}$ triple bonds. The metallacyclic portion in **6** features longer $\text{Ru}(2)-\text{C}(14)$ [2.154(2) Å] and $\text{C}(13)-\text{C}(14)$ bonds [1.357(4) Å] consistent with the presence of $\text{Ru}-\text{C}$ single and $\text{C}=\text{C}$ double bonds. The $\text{C}(13)=\text{C}(14)$ double bond adopts the more thermodynamically stable *E* configuration, and is coplanar with its substituents $\text{C}(131)$, $\text{C}(12)$, $\text{C}(15)$ and $\text{Ru}(2)$.

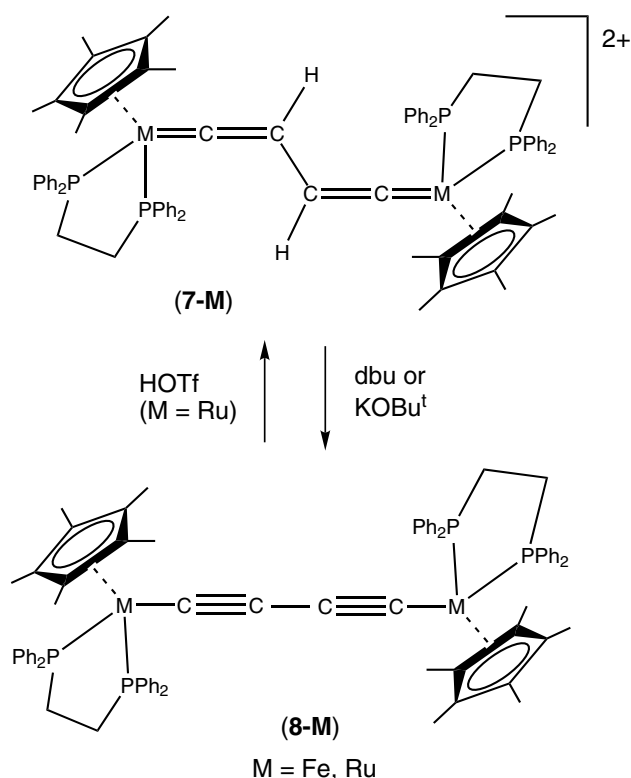
2.4. Protonation of $\{\text{Ru}(\text{dppe})\text{Cp}^*\}_2(\text{CCCC})$ (**8**)

The bis-vinylidenes $[\{\text{M}(\text{dppe})\text{Cp}^*\}_2(=\text{C}=\text{CHCH}=\text{C}=\text{C})]^{2+}$ (**7-M** = Fe [2], Ru [3], Os [4]) can all be doubly deprotonated to give the corresponding diyndiyl complexes. However, the reverse reaction involving the protonation of the diyndiyl complexes to give the bis-vinylidenes has not been demonstrated. The addition of triflic acid to a solution of the iron diyndiyl $\{\text{Fe}(\text{dppe})\text{Cp}^*\}_2(\text{C}\equiv\text{CC}\equiv\text{C})$ (**8-Fe**) gave multiple products that presently have not been characterised [16]. So, while trivial in concept, protonation of the diyndiyl complex **8-Ru** was investigated.

Addition of a slight excess of triflic acid to a CH_2Cl_2 solution of **8-Ru** resulted in a rapid colour change from orange to deep red. The reaction mixture was stirred for 30 min before diethyl ether was added to crystallise the product, which was shown to be $[\{\text{Ru}(\text{dppe})\text{Cp}^*\}_2(=\text{C}=\text{CHCH}=\text{C}=\text{C})](\text{OTf})_2$ (**7-Ru/OTf**) by comparison with an authentic sample (Scheme 5). The IR spectrum contained a single $\nu(\text{C}=\text{C})$ band at 1600 cm^{-1} , while the ^1H and ^{31}P NMR spectra were similar to those found earlier for $[\{\text{Ru}(\text{dppe})\text{Cp}^*\}_2\{\mu(=\text{C}=\text{CHCH}=\text{C}=\text{C})\}](\text{PF}_6)_2$ (**7-Ru/PF₆**) [3b].

2.5. Oxidation to $[\text{Ru}(\text{CO})(\text{dppe})\text{Cp}^*]\text{PF}_6$ (**9**)

While bis(vinylidene) complexes are all air-stable solids, decomposition was observed if solutions were left



Scheme 5.

exposed to air (1–2 days). The carbonyl cation $[\text{Ru}(\text{CO})(\text{dppe})\text{Cp}^*]\text{PF}_6$ (**9**) was isolated from aged solutions as the major decomposition product. It was identified by comparison with the literature [17], with $\nu(\text{CO})$ at 1972 cm^{-1} and NMR resonances at δ_{H} 1.66 (Cp*) and δ_{C} 10.20 (Cp*–Me), 100.05 (Cp*–ring) and 203.31 (CO). Similar oxidations of Ru(II) vinylidenes to give carbonyl cations have previously been reported and in some cases aldehyde by-products isolated [10,18–21]. An alternative synthesis of **9** was by the direct reaction of **1** with $[\text{NH}_4]\text{PF}_6$ in MeOH under an atmosphere of CO. The solution gradually changed colour from bright orange to a very pale yellow upon completion of the reaction.

Crystals were obtained directly from an oxidised solution of **5** in MeOH and proved to consist of the mono-MeOH solvate, **9**·MeOH. Crystals from CH_2Cl_2 -Et₂O were solvent-free. The structural determinations of both gave bond parameters which were essentially identical, values for the latter being cited in the following. A view of the cation is shown in Fig. 2 and selected structural parameters of both forms are collected in the caption. Coordination about the Ru atom is similar to that found in the other complexes described above $[\text{Ru}-\text{C}(\text{Cp}^*)]$ (av.) 2.27(2), Ru–P 2.3220, 2.3315(5), Ru–CO 1.859(2) Å; P(1)–Ru–P(2) 83.01(2)°, P(1,2)–Ru–CO 88.63°, 92.53(6)°. The two Ru–P dis-

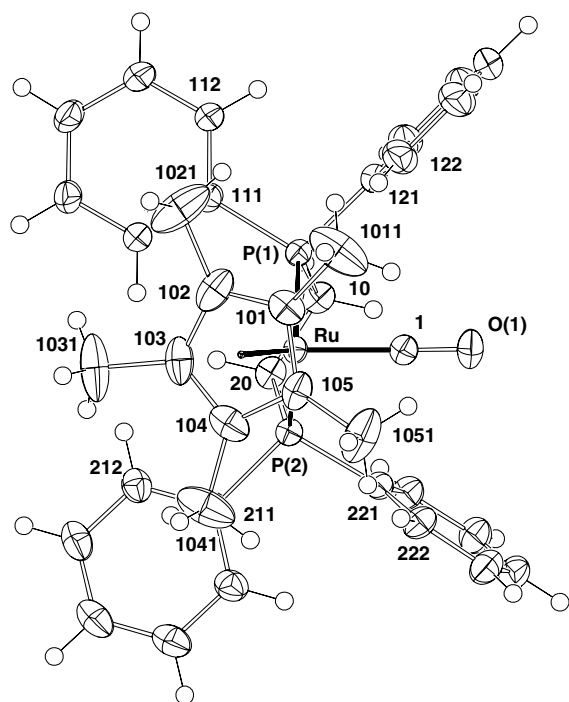


Fig. 2. Projection of the cation in $[\text{Ru}(\text{CO})(\text{dppe})\text{Cp}^*]\text{PF}_6$ (**9**). Bond distances (Å) in **9**·MeOH: Ru–P(1) 2.3220(5), 2.3188(5); Ru–P(2) 2.3315(5), 2.3311(4); Ru–C(Cp*) 2.228–2.289(2), 2.251–2.298(2), (av.) 2.26(3), 2.27(2); Ru–C(1) 1.859(2), 1.857(2). Bond angles (°): P(1)–Ru–P(2) 83.01(2), 83.06(2); P(1)–Ru–C(1) 88.63(6), 83.90(7); P(2)–Ru–C(1) 92.53(6), 91.32(7).

tances are slightly longer than in $\text{RuCl}(\text{dppm})\text{Cp}^*$ [2.2882(5), 2.2812(4) Å] [3b] and reflect the reduced back-bonding from the cationic ruthenium centre to the phosphorus nuclei. The carbonyl group has similar Ru–C and C–O bond lengths to those found in related complexes [20,22].

2.5.1. Electrochemistry

The bis-ruthenium complexes **5** and **6** were further investigated by cyclic voltammetry. In the case of **5**, two fully reversible waves were observed at $E_{1/2} = +0.82$ and $+1.20$ V (referenced to $\text{FcCp}_2/[\text{FcCp}_2]^+ = +0.46$ V). Comparisons show that **5** is thermodynamically easier to oxidise than the related hydrogen analogue **4** ($E_{1/2} = +1.00$ and $+1.26$ V). Additionally, the separation between the two waves (ΔE) is greater in **5** (380 mV) than in **4** (260 mV), suggesting that the methyl groups at the C₂ positions in **5** have enhanced the electronic interactions between the two ruthenium centres by donating electron density into the HOMOs which are expected to extend between the two ruthenium centres. This large interaction is also indicated by the large comproportionation constant, $K_c = 2.64 \times 10^6$.

The asymmetric complex **6** revealed two reversible well-separated waves at $E_{1/2} = -0.30$ and $+0.04$ V, corresponding to the sequential oxidation of each ruthenium from Ru(II) to Ru(III). Evaluation of the electronic interactions across the bridging ligand in this case is difficult, as comparisons need to be made for the corresponding symmetric derivatives, which for the metallocyclic complexes have yet to be prepared.

3. Conclusions

We have shown above that ruthenium(II) vinylidenes containing a coordinated dpmm ligand transform to new metallocyclic structures by a reaction sequence which probably involves deprotonation of the dpmm ligand followed by intramolecular attack of the resulting anion at C₁. In the case of the methylated bis-vinylidene **5**, treatment with KO^tBu resulted in deprotonation of a single dpmm ligand and cyclisation together with removal of a methyl group to form the metallocyclic and ethynyl portions found in **6**, respectively. The single-crystal X-ray structures of **3** and **6** confirm the formation of a 1-ruthena-2,4-diphosphabicyclo[1.1.1]pentane moiety in each case.

Despite the protonation of the iron diynyl complex **8-Fe** yielding a mixture of inseparable products, the reaction of **8-Ru** with a twofold excess of HOTf gave the expected bis-vinylidene **7-Ru/OTf** as the sole product. However, care must be taken while handling **7-Ru** and related complexes in solution to prevent their oxidation to $[\text{Ru}(\text{CO})(\text{dppe})\text{Cp}^*]^+$.

4. Experimental

4.1. General experimental conditions

All reactions were carried out under dry, high purity argon using standard Schlenk techniques. Common solvents were dried, distilled under argon and degassed before use.

4.2. Instrumentation

Infrared spectra were obtained on a Bruker IFS28 FT-IR spectrometer. Spectra in CH₂Cl₂ were obtained using a 0.5 mm path-length solution cell with NaCl windows. Nujol mull spectra were obtained from samples mounted between NaCl discs. NMR spectra were recorded on Bruker AM300WB or ACP300 (¹H at 300.13 MHz, ¹³C at 75.47 MHz, ³¹P at 121.503 MHz) instruments. Samples were dissolved in CDCl₃, unless otherwise stated, contained in 5 mm sample tubes. Chemical shifts are given in ppm relative to internal tetramethylsilane for ¹H and ¹³C NMR spectra and external H₃PO₄ for ³¹P NMR spectra. ES mass spectra: VG Platform 2 or Finnigan LCQ. Solutions were directly infused into the instrument. Chemical aids to ionisation were used as required [23]. Cyclic voltammograms were recorded using a PAR model 263 apparatus, a saturated calomel electrode, and ferrocene as internal calibrant ([FeCp₂]/[FeCp₂]⁺ = +0.46 V). Elemental analyses were performed at the Centre pour Microanalyses du CNRS, Vernaison, France, and CMAS, Belmont, Australia.

4.3. Reagents

Compounds **1**, **2** and **8-Ru** were prepared using the methods previously reported [3b].

4.4. Treatment of

[{Ru(dppm)Cp*}₂(=C=CHCH=C=)](PF₆)₂ (**1**) with KOBu^t

To a solution of **1** (50 mg, 0.03 mmol) in THF (20 mL) was added KOBu^t (10.6 mg, 0.09 mmol). The reaction mixture was left to stir at r.t. for 10 min before the solvent was removed. The orange residue was extracted into hexane and the solution filtered and concentrated under vacuum to give a bright orange solid (40 mg), identified by NMR as a mixture of three complexes: {Ru(dppm)Cp*}₂(μ-C≡CC≡C) (**2**) (35%). ¹H NMR: δ 1.90 (s, 30H, Cp*), 4.22 (m, 4H, CH₂). ³¹P NMR: δ 16.63 (s, dppm); Ru{C≡CCH=CCH(PPh₂)₂[RuCp*]}(dppm)Cp* (**3**) (60%). ¹H NMR: δ 1.98 [t, J(HP) 2 Hz, 15H, Cp*], 2.07 [t, J(HP) 1 Hz, 15H, Cp*], 2.11 (s, 1H, =CH), 3.85, 4.12 (m, 2H, CH₂), 5.59 [t, J(HP) 4 Hz, 1H, P₂CH]. ³¹P NMR: δ -1.80 (s, P₂CH), 18.99 (s, dppm); {Ru[(PPh₂)₂CHC=CH-

]Cp*₂ (**4**) (5%). ¹H NMR: δ 2.24 (s, 30H, Cp*), 6.43 (br, 2H, P₂CH). ³¹P NMR: δ -3.05 (s, P₂CH).

4.5. [{Ru(dppm)Cp*}₂(=C=CMeCMe=C=)](OTf)₂ (**5**)

To a solution of **2** (500 mg, 0.38 mmol) in CH₂Cl₂ (25 mL) was added MeOTf (0.096 mL, 0.84 mmol, 2.2 equiv). The solution was stirred at r.t. for 3 h, gradually changing in colour from orange to green. Diethyl ether (50 mL) was added and the bright green product crystallised. The solid was filtered and washed with THF and diethyl ether to give [{Ru(dppm)Cp*}₂(=C=CMeCMe=C=)](OTf)₂ (**5**) (390 mg, 63%). Anal. Calc. (C₇₈H₈₀F₆O₆P₄Ru₂S₂): C, 57.92; H, 4.98; M (cation), 1320. Found: C, 58.01; H, 4.86%. IR (Nujol, cm⁻¹): ν(C=C) 1626 m. ¹H NMR (acetone-*d*₆): δ 0.06 (s, 6H, 2 × Me), 1.98 (s, 30H, Cp*), 4.82, 5.32 (2m, 2 × 2H, CH₂), 7.22–7.61 (m, 40H, Ph). ¹³C NMR (acetone-*d*₆): δ 8.75 (s, Me), 12.37 (s, C₅Me₅), 45.77 [t, J(CP) 27 Hz, CH₂], 104.61 (s, C₅Me₅), 117.45 (s, C₂), 129.96–136.81 (m, Ph), 352.20 [t, J(CP) 14 Hz, C₁]. ³¹P NMR (acetone-*d*₆): δ 2.00 (s, dppm). ES-mass spectrum (*m/z*): 1469, [M + OTf]⁺; 660, [M]²⁺.

4.6. Ru{CCCH=CH(PPh₂)₂[Rucp*]}(dppm)Cp* (**6**)

To a suspension of **5** (70 mg, 0.04 mmol) in THF (10 mL) was added KOBu^t (19.4 mg, 0.17 mmol). The reaction was left to stir at r.t. for 10 min before the solvent was removed and the orange solid extracted into hexane. The solution was filtered and concentrated under vacuum to give bright orange crystals identified as Ru{C≡CCH=CH(PPh₂)₂[RuCp*]}(dppm)Cp* (**6**) (44 mg, 78%). Anal. Calc. (C₇₅H₇₆P₄Ru₂): C, 69.11; H, 5.88; M, 1304. Found: C, 69.14; H, 5.91%. IR (Nujol, cm⁻¹): ν(C≡C) 1950 w; ν(C=C) 1713 m. ¹H NMR (benzene-*d*₆): δ 1.97 (s, 15H, Cp*), 1.99 [t, J(HP) 12 Hz, 3H, Me], 2.22 (s, 15H, Cp*), 3.94, 4.25 (2m, 2 × 1H, CH₂), 5.43 [t, J(HP) 4 Hz, 1H, PCHP], 6.78–7.73 (m, 40H, Ph). ¹³C NMR (toluene-*d*₈): δ 11.42 (s, C₈), 13.15 (s, C₁₀), 27.87 [t, J(CP) 7 Hz, C₅], 29.94 (s, C₃₁), 49.79 [t, J(CP) 22 Hz, C₆], 72.54 [t, J(CP) 23 Hz, C₃], 87.85 [t, J(CP) 2 Hz, C₉], 91.28 [t, J(CP) 2 Hz, C₇], 113.54 [t, J(CP) 11 Hz, C₂], 116.84 [tt, J(CP) 25 Hz, J(CP) 5 Hz, C₁], 126.30–139.10 (m, Ph), 203.24 (s, C₄). ³¹P NMR (benzene-*d*₆): δ 0.49 (s, P₂CH), 19.05 (s, dppm). ES-mass spectrum (*m/z*): 1336, [M + MeOH]⁺; 1305, [M + H]⁺.

4.7. [{Ru(dppe)Cp*}₂(=C=CHCH=C=)](OTf)₂ (**7-Ru/OTf**)

To a solution of {Ru(dppe)Cp*}₂(C≡CC≡C) (**8-Ru**) (100 mg, 0.07 mmol) in CH₂Cl₂ (10 mL) was added HOTf (0.015 mL, 0.17 mmol, 2.2 equiv). The reaction

was stirred at r.t. for 15 min before diethyl ether (50 mL) was added. The brick red crystals were filtered and washed with further portions of diethyl ether to give $[\{\text{Ru}(\text{dppe})\text{Cp}^*\}_2(\text{C}=\text{CHCH}=\text{C}=\text{C})](\text{OTf})_2$ (**7-Ru/OTf**) (88 mg, 72%). IR (Nujol, cm^{-1}): $\nu(\text{C}=\text{C})$ 1600 m. ^1H NMR: δ 1.66 (s, 30H, Cp*), 2.57–2.78 (m, 8H, CH_2CH_2), 3.13 (s, 2H, =CH), 7.00–7.56 (m, 40H, Ph). ^{31}P NMR: δ 75.92 (s, dppe).

4.8. $[\text{Ru}(\text{CO})(\text{dppe})\text{Cp}^*]\text{PF}_6$ (**9**)

A solution of **1** (100 mg, 0.15 mmol) and $[\text{NH}_4]\text{PF}_6$ (49 mg, 0.30 mmol) in methanol (20 mL) was stirred at room temperature overnight under 1 bar of CO giving a pale yellow solution. The solvent was removed under vacuum and the solid was extracted in a minimum quantity of CH_2Cl_2 and filtered dropwise into rapidly stirred Et_2O (100 mL). The solid product was collected on a sintered glass funnel and washed with pentane to give pale yellow crystals of $[\text{Ru}(\text{CO})(\text{dppe})\text{Cp}^*]\text{PF}_6$ (**9**) (108 mg, 90%). IR (CH_2Cl_2) $\nu(\text{CO})$ 1972 cm^{-1} . ^1H NMR (CDCl_3) δ_{H} 7.17–7.61 (m, 20H, Ph), 2.62, 2.71 (2m, 4H, CH_2CH_2), 1.66 (s, 15H, Cp*). ^{13}C NMR (CDCl_3) δ_{C} 203.31 (s, CO), 129.48–133.55 (m, Ph), 100.05 (s, Cp*), 30.14 (m; CH_2CH_2), 10.20 (s, Cp*). ^{31}P NMR (CDCl_3) δ_{P} 72.72 (dppe), –143.05 (septet, PF_6). [Lit. values: $^{17}\nu(\text{CO})$ 1975s cm^{-1} . ^1H NMR: δ 1.62 (m), 2.60–2.80 (m), 7.08–7.58 (m). ^{13}C NMR: δ 9.6 (s), 29.6–30.2 (m), 99.4 (s), 128.7–132.3 (m), 202.7 [t, $J(\text{CP})$ 16]. ^{31}P NMR: δ 70.4 (s)]. A second X-ray sample was ob-

tained from MeOH and formed a mono-methanol solvate (**9 · MeOH**).

5. Crystallography

Full spheres of diffraction data were measured at ca. 153 K using a Bruker AXS CCD area-detector instrument. N_{tot} reflections were merged to N unique (R_{int} quoted) after “empirical”/multiscan absorption correction (proprietary software), N_{o} with $F > 4\sigma(F)$ being used in the full matrix least squares refinement. All data were measured using monochromatic Mo $\text{K}\alpha$ radiation, $\lambda = 0.71073$ Å. Anisotropic thermal parameter forms were refined for the non-hydrogen atoms, $(x, y, z, U_{\text{iso}})_{\text{H}}$ being constrained at estimated values. Conventional residuals R , R_w on $|F|$ are given [weights: $\sigma^2(F) + 0.000n_w(F^2)^{-1}$]. Neutral atom complex scattering factors were used; computation used the XTAL 3.7 program system [24]. Pertinent results are given in the figures (which show non-hydrogen atoms with 50% probability amplitude displacement envelopes and hydrogen atoms with arbitrary radii of 0.1 Å) and Tables 1 and 2.

5.1. Variata

Compound 4. Weak and limited data would support meaningful anisotropic displacement parameter refinement for Ru, P, Cl only. In particular, residues modelling solvent molecules displayed very high

Table 2
Crystal data and refinement details

Compound	4	5	6	9	9 · MeOH
Formula	$\text{C}_{74}\text{H}_{74}\text{P}_4\text{Ru}_2 \cdot 2\text{CH}_2\text{Cl}_2$	$\text{C}_{78}\text{H}_{80}\text{F}_6\text{O}_6\text{P}_4\text{Ru}_2\text{S}_2 \cdot 3.62\text{CH}_2\text{Cl}_2$	$\text{C}_{75}\text{H}_{76}\text{P}_4\text{Ru}_2 \cdot \text{C}_5\text{H}_{12}$	$\text{C}_{37}\text{H}_{39}\text{F}_6\text{OP}_3\text{Ru}$	$\text{C}_{37}\text{H}_{39}\text{F}_6\text{OP}_3\text{Ru} \cdot \text{CH}_4\text{O}$
Molecular weight	1459.3	1925.8	1375.6	807.7	839.7
Crystal system	Monoclinic	Triclinic	Triclinic	Monoclinic	Monoclinic
Space group	$P2_1/c$	$P\bar{1}$	$P\bar{1}$	$P2_1/c$	$P2_1/n$
a (Å)	36.157(8)	11.5467(7)	14.956(2)	14.3025(8)	11.8060(7)
b (Å)	12.626(3)	12.0389(8)	22.161(3)	15.4394(8)	17.024(1)
c (Å)	23.613(5)	16.902(1)	22.408(3)	16.9174(9)	18.696(1)
α (°)		73.304(2)	102.687(3)		
β (°)	94.468(5)	74.867(2)	101.318(3)	110.075(2)	103.486(1)
γ (°)		71.343(2)	100.315(3)		
V (Å ³)	10747	2095	6910	3509	3654
Z	6	1	4	4	4
D_c (g cm ⁻³)	1.35 ₃	1.52 ₆	1.32 ₂	1.52 ₉	1.52 ₆
μ (cm ⁻¹)	7.0	0.78	0.57	0.65	6.3
Crystal size (mm)	0.15 × 0.13 × 0.04	0.28 × 0.24 × 0.14	0.28 × 0.20 × 0.14	0.35 × 0.18 × 0.14	0.20 × 0.14 × 0.12
$T_{\text{min/max}}$	0.83	0.86	0.74	0.88	0.83
$2\theta_{\text{max}}$ (°)	58	75	75	75	75
N_{tot}	106 511	43 312	92 460	71 458	64 785
N_r (R_{int})	27 653 (0.13)	21 525 (0.039)	63 824 (0.044)	18 410 (0.033)	18 312 (0.043)
N_{o}	10 379	14 077	38 872	13 335	13 233
R	0.086	0.049	0.050	0.043	0.040
R_w (n_w)	0.091 (5)	0.052 (5)	0.060 (8)	0.058 (10)	0.044 (4)

displacement parameters and solvents 3, 4 were assigned site occupancies of 0.5 after trial refinement.

Compound 5. The hydrocarbon composite between the two ruthenium atoms and beyond C(1) was modelled in terms of a pair of disordered components, site occupancies refining to 0.624(8) and complement. The anion was modelled in terms of a pair of disordered components, site occupancies refining to 0.815(2) and complement, in concert with a pair of nearby solvent molecule components, the minor residues being refined with isotropic displacement parameter forms.

Compound 6. $l = 2n + 1$ reflections are very weak, the superlattice most noticeably manifest in the orientation of ring 112n cf. ring 312n in the resulting model.

Compound 9. The fluorine atoms of the anion were modelled as disordered over two sets of sites, occupancies refining to 0.789(4) and complement.

Compound 9 · MeOH. The MeOH hydroxyl hydrogen was not located; the atom assigned as oxygen lies 2.884(4), 2.981(3) Å from F(1, 5) of the anion.

6. Supplementary material

Full details of the structure determinations (except structure factors) have been deposited with the Cambridge Crystallographic Data Centre as CCDC Nos. 246286–246288 (complexes **4–6**), 246472 (**9**) and 246473 (**9 · MeOH**). Copies of this information may be obtained free of charge from The Director, CCDC, 12 Union Road, Cambridge CB2 1EZ, UK (fax: +44 1223 336 033; e-mail: deposit@ccdc.cam.ac.uk or www: <http://www.ccdc.cam.ac.uk>).

Acknowledgements

Mass spectra were obtained with the kind assistance of Professor B.K. Nicholson (University of Waikato, Hamilton, New Zealand). We thank the Australian Research Council for support of this work and Johnson Matthey plc, Reading, UK, for a generous loan of $\text{RuCl}_3 \cdot n\text{H}_2\text{O}$.

References

- [1] P.J. Low, M.I. Bruce, *Adv. Organomet. Chem.* 48 (2001) 71.
- [2] (a) N. Le Narvor, C. Lapinte, *J. Chem. Soc., Chem. Commun.* 357 (1993);
(b) N. Le Narvor, L. Toupet, C. Lapinte, *J. Am. Chem. Soc.* 117 (1995) 7129;
(c) F. Coat, C. Lapinte, *Organometallics* 15 (1996) 477;
(d) N. Le Narvor, C. Lapinte, *C.R. Acad. Sci. Paris, Ser. II* 1 (1998) 745.
- [3] (a) P.J. Low, K. Costuas, J.-F. Halet, S.P. Best, G.A. Heath, *J. Am. Chem. Soc.* 122 (2000) 1949;
(b) M.I. Bruce, B.G. Ellis, P.J. Low, B.W. Skelton, A.H. White, *Organometallics* 22 (2003) 3184.
- [4] M.I. Bruce, K.A. Kramarczuk, unpublished work.
- [5] M.I. Bruce, B.G. Ellis, M. Gaudio, C. Lapinte, G. Melino, F. Paul, B.W. Skelton, M.E. Smith, L. Toupet, A.H. White, *Dalton Trans.* (2004) 1601.
- [6] (a) M.I. Bruce, A.G. Swincer, *Adv. Organomet. Chem.* 22 (1983) 59;
(b) M.I. Bruce, *Chem. Rev.* 91 (1991) 197.
- [7] H. Werner, *J. Organomet. Chem.* 475 (1994) 44.
- [8] M.C. Puerta, P. Valerga, *Coord. Chem. Rev.* 193–195 (1999) 977.
- [9] (a) N.M. Kostic, R.F. Fenske, *Organometallics* 1 (1982) 974;
(b) J. Silvestre, R. Hoffmann, *Helv. Chim. Acta* 68 (1985) 1461;
(c) O.F. Koentjoro, R. Rousseau, P.J. Low, *Organometallics* 20 (2001) 4502;
(d) N. Auger, D. Touchard, S. Rigaut, J.-F. Halet, J.-Y. Saillard, *Organometallics* 22 (2003) 1638.
- [10] M.I. Bruce, A.G. Swincer, R.C. Wallis, *J. Organomet. Chem.* 171 (1979) C5.
- [11] S.G. Davies, A.J. Smallridge, *J. Organomet. Chem.* 395 (1990) C39.
- [12] M.I. Bruce, D.N. Duffy, M.G. Humphrey, A.G. Swincer, *J. Organomet. Chem.* 282 (1985) 383.
- [13] (a) M.P. Gamasa, J. Gimeno, E. Lastra, B.M. Martin, A. Aguirre, S. Garcia-Granda, P. Pertierra, *J. Organomet. Chem.* 429 (1992) C19;
(b) V. Cadierno, M.P. Gamasa, J. Gimeno, B.M. Martin-Vaca, *J. Organomet. Chem.* 617–618 (2001) 261.
- [14] M.I. Bruce, M.P. Cifuentes, M.G. Humphrey, E. Poczman, M.R. Snow, E.R.T. Tiekink, *J. Organomet. Chem.* 338 (1988) 237.
- [15] R.D. Adams, A. Davison, J.P. Selegue, *J. Am. Chem. Soc.* 101 (1979) 7232.
- [16] C. Lapinte, personal communication, 2002.
- [17] F.M. Conroy-Lewis, S.J. Simpson, *J. Organomet. Chem.* 322 (1987) 221.
- [18] L.A. Oro, M.A. Ciriano, M. Campo, C. Foces-Foces, F.H. Cano, *J. Organomet. Chem.* 289 (1985) 117.
- [19] A. Mezzetti, G. Consiglio, F. Morandini, *J. Organomet. Chem.* 430 (1992) C15.
- [20] R. Le Lagadec, E. Roman, L. Toupet, U. Mueller, P.H. Dixneuf, *Organometallics* 13 (1994) 5030.
- [21] C. Bianchini, P. Innocenti, M. Peruzzini, A. Romerosa, F. Zanobini, *Organometallics* 15 (1996) 272.
- [22] I. de los Rios, M.J. Tenorio, M.C. Puerta, P. Valerga, *J. Organomet. Chem.* 549 (1997) 221.
- [23] W. Henderson, J.S. McIndoe, B.K. Nicholson, P.J. Dyson, *J. Chem. Soc., Dalton Trans.* (1998) 519.
- [24] S.R. Hall, D.J. du Boulay, R. Olthof-Hazekamp (Eds.), *The X-TAL 3.7 System*, University of Western Australia, Perth, 2000.